Statistical Distribution of Beamforming Gains in Satellite Swarms Under Imperfect Phase Synchronization

Biniam Tamiru, Konstantinos Ntontin, Liz Martinez Marrero, and Symeon Chatzinotas
Interdisciplinary Centre for Security, Reliability and Trust (SnT), University of Luxembourg,
Emails: {biniam.tamiru, kostantinos.ntontin, liz.martinez-marrero, symeon.chatzinotas}@uni.lu

***Abstract*—In this paper, we analytically study the distribution of the main-lobe gain in a low-Earth orbit (LEO) satellite swarm scenario under imperfect phase synchronization, based on an open-loop process. The provided analytical framework determines the maximum tolerable error in phase estimation under which the desired beamforming gain can still be achieved. Consequently, we are able to determine the highest value of accuracy (worst-case scenario) in position estimation between satellites (inter-node ranging) required for phase synchronization. Notably, the analytical framework reveals that in millimeter-wave bands, the required maximum precision in inter-node ranging to guarantee just a small performance deterioration is in the order of millimetres. Finally, numerical results based on Monte Carlo simulations validate the analytical framework.**

***Index Terms*—LEO-satellites, phase error, beamforming gain**

I. Introduction

A. Background

The amalgamation of terrestrial with non-terrestrial networks (NTNs) has been an area of intense investigation over the last years due to the capability of the latter networks to provide ubiquitous coverage. They are the only viable way from a cost and energy-efficiency perspective for facilitating remote/rural areas that lack adequate terrestrial infrastructure [1]. However, achieving an adequate gain from space to counteract the large distances to Earth and realize broadband communication for handheld devices, so as to provide similar quality of service with the one achieved by terrestrial urban infrastructure, is severely restricted by the size of the satellites in low-Earth orbit (LEO). Launching large monolithic apertures from ground to achieve the required gain is not a desirable approach due to the resulting costs. Instead, to abide by the trend of satellite miniaturization for reducing the costs and making future satellite networks sustainable, satellite cooperation for achieving a high beamforming gain towards a handheld user on ground, through distributed beamforming, has been proposed as a notably more cost-effective solution [2], [3].

As far as geometry aspects are concerned, a satellite swarm can be arranged in a geometry that suits the specific design and is manageable with respect to affordable computational resources and control systems. Moreover, the distributed satellite coordination process renders necessary to provide solutions for the effective synchronization of the swarm in time, frequency, and phase [4], [5]. Closed loop systems deploy an external to the swarm node, such as the targeted receiver, a ground station, or an additional satellite, to achieve coherent beamforming through continuous feedback from the external node. Hence, the satellites are not required to communicate with each other. On the other hand, in open-loop systems the satellites achieve synchronization based on communication only within the swarm [6].

Among time, frequency, and phase synchronization, the latter could be the most challenging one depending on the frequency of operation. For instance, a mm accuracy level in the inter-satellite ranging process can be required so that the distributed beamforming operation does not get out of coherence. For terrestrial systems with stationary distributed nodes, [7]–[9] compute the average beamforming gains under and imperfect phase synchronization assumption. Furthermore, in the satellite domain, for a swarm formation arranged in a square geometry and a phase synchronization error that follows the uniform distribution the authors in [10] provide plots for the effect of different magnitudes of the phase imperfections on the swarm radiation pattern by generating random realizations. However, apart from the average distributed beamforming gains under imperfect phase synchronization, equally important for the system designer is the computation of the distribution of the main-lobe gain due to the randomness in the phase synchronization. This is something that is largely missing from the literature, but it is very important for the system designer since it can reveal more important trends than the average value. For instance, the effect of an increasing number of satellites on the shape of the main lobe gain distribution can be better investigated.

B. Motivation and contribution

Based on the previous discussion, it becomes clear that an analytical framework for the distribution of the main-lobe gain in satellite swarms that perform distributed beamforming under phase synchronization errors is missing. This is essential so that the system designer does not resort to time-consuming simulations for several parameters of interest. Moreover, the time complexity for such simulations increases rapidly as the number of satellites increases. Through the aforementioned framework an analytical determination of the phase error

tolerance to achieve a certain quality of service would give a performance benchmark for inter-satellite ranging algorithms, which are essential in open-loop satellite systems.

Given the aforementioned limitations in the literature, our contribution in this work can be summarized as follows:

- For a satellite swarm scenario we compute the probability distribution function of normalized main lobe gain under the assumption that random independent phase errors are introduced to each of the satellites.
- Based on the probability distribution, we compute the maximum tolerable phase error bound (in the assumed error distribution) so that the probability of not achieving the nominal target data rate does not exceed a certain threshold. This, in turn, allows us to determine the maximum inter-satellite ranging accuracy needed for different carrier frequencies so that the requirements are met.

The results of the mentioned analysis are validated by Monte Carlo simulations.

The remainder of this work is organized as follows: Section II introduces the system model, Section III lays the analytical derivations needed to compute the maximum tolerable phase error, whereas Section IV presents the numerical results obtained and their implications. Finally, Section V concludes this work with the main takeaways and potential ideas for future work.

II. System model

We consider S satellites, each equipped with N antennas, and arranged in an arbitrary geometry. Let $\mathbf{u}_s(n) = [x_s + x_n, y_s + y_n, z_s + z_n]$ be the position of antenna n in satellite s, where $[x_s, y_s, z_s]$ is the position of the center of satellite s and $[x_n, y_n, z_n]$ is the position of antenna n with respect to the satellite center. The wave vector is defined as $k(\varphi, \theta) = \frac{2\pi}{\lambda}[\cos\theta\cos\varphi,\ \cos\theta\sin\varphi,\ \sin\theta]$.

In addition, we model the phase error in the synchronization process of the satellites as a random variable, denoted by ϕ_s. Without loss of generality, in this work we consider a uniform distribution, similar to [10]. Hence, $\phi_s \sim U(-\phi, \phi)$. It has been shown in [10] that the received power along the azimuth and elevation angles of φ and θ, respectively, is given by

$$\zeta(\varphi,\theta) = \left| \frac{1}{g(\theta)\sqrt{NS}} \mathbf{a}^H(0,0)\mathbf{a}(\varphi,\theta,\Phi) \right|^2, \tag{1}$$

where
$\mathbf{a}(\varphi,\theta,\Phi) = \left[\left(e^{j\phi_1}\mathbf{a}_1(\varphi,\theta)\right)^T, \ldots, \left(e^{j\phi_S}\mathbf{a}_S(\varphi,\theta)\right)^T \right]$,
$\mathbf{a}_s(\varphi,\theta) = g(\theta)\left[e^{jk^T(\varphi,\theta)\mathbf{u}_s(1)}, \ldots, e^{jk^T(\varphi,\theta)\mathbf{u}_s(N)}\right]^T$
Substituting these expressions into (1), we get

$$\zeta(\varphi,\theta) = \left| \frac{g(\theta)}{\sqrt{NS}} \sum_{s=1}^{S} e^{j\left[\frac{2\pi}{\lambda}((\Theta-1)x_s+\psi y_s+\Omega z_s)+\phi_s\right]} \times \sum_{n=1}^{N} e^{j\frac{2\pi}{\lambda}[(\Theta-1)x_n+\psi y_n+\Omega z_n]} \right|^2 \tag{2}$$

where $\Theta = \cos\theta\cos\varphi$, $\Omega = \sin\theta$, and $\Psi = \cos\theta\sin\varphi$. If we consider the main-lobe gain, $\theta = \varphi = 0$, (2) reduces to

$$\zeta(0,0) = g(0)^2 \frac{N}{S} \left| \sum_{s=1}^{s=S} e^{j\phi_s} \right|^2, \tag{3}$$

as implied in [10]. In the special case where $\phi_s = 0$, the maximum gain with perfect phase synchronization is achieved.

$$\zeta_{max}(0,0) = g(0)^2 NS \tag{4}$$

III. Analysis

A. Distribution of the main lobe gain

We will now analyze the characteristics of the main lobe gain under a uniformly distributed ϕ_s described above, and derive closed-form expression for its cumulative distribution function (CDF). According to (1), the relative gain with respect to the maximum gain, which we denote by G_ϕ, is given by

$$G_\phi = \frac{\zeta(0,0)}{\zeta_{max}(0,0)} = \left(G_\phi{}^{real}\right)^2 + \left(G_\phi{}^{img}\right)^2, \quad 0 \le G_\phi \le 1 \tag{5}$$

where $G_\phi{}^{real} = \frac{\sum_{s=1}^{s=S}\cos(\phi_s)}{S}$ and $G_\phi{}^{img} = \frac{\sum_{s=1}^{s=S}\sin(\phi_s)}{S}$.

We now start by making simplifying assumptions regarding the nature of the distribution of $G_\phi{}^{real}$ and $G_\phi{}^{img}$, and the relationship between them. The central limit theorem dictates that for sufficiently large S, the sum of independent and identically distributed (i.i.d) random variables approaches a Gaussian distribution [11]. Consequently, the following approximations hold

$$\begin{aligned} \sqrt{S}\left(G_\phi{}^{real} - \mu_\phi{}^{real}\right) &\sim N\left(0, \sigma^2_{\cos\phi_s}\right) \\ \sqrt{S}\left(G_\phi{}^{img} - \mu_\phi{}^{img}\right) &\sim N\left(0, \sigma^2_{\sin\phi_s}\right), \end{aligned} \tag{6}$$

where $\sigma^2_{\cos\phi_s}$ and $\sigma^2_{\sin\phi_s}$ are the variances of $\cos\phi_s$ and $\sin\phi_s$ respectively.

Lemma 1: We define $\mu_\phi{}^{real}$ and $\left(\sigma_\phi{}^2\right)^{real}$ as the mean and variance of $G_\phi{}^{real}$, whereas $\mu_\phi{}^{img}$ and $\left(\sigma_\phi{}^2\right)^{img}$ as the mean and variance of $G_\phi{}^{img}$. Then, it holds that

$$\mu_\phi{}^{real} = \frac{\sin(\phi)}{\phi}, \quad \mu_\phi{}^{img} = 0 \tag{7}$$

$$\left(\sigma_\phi{}^2\right)^{real} = \frac{1}{S}\left[\frac{1}{2} + \frac{\sin(2\phi)}{4\phi} - \left(\frac{\sin(\phi)}{\phi}\right)^2\right]$$

$$\left(\sigma_\phi{}^2\right)^{img} = \frac{1}{S}\left[\frac{1}{2} - \frac{\sin(2\phi)}{4\phi}\right], \tag{8}$$

Proof: See Appendix A.
We can now re-write (5) as follows:

$$G_\phi = \left(\sigma_\phi{}^2\right)^{real}\left(\frac{G_\phi{}^{real}}{(\sigma_\phi)^{real}}\right)^2 + \left(\sigma_\phi{}^2\right)^{img}\left(\frac{G_\phi{}^{img}}{(\sigma_\phi)^{img}}\right)^2 \tag{9}$$

G_ϕ is expressed as the linear combination of the squares of Gaussian random variables normalized to a unit standard deviation. It holds that $\left(\frac{{G_\phi}^{img}}{({\sigma_\phi})^{img}}\right)^2$ has a chi-square distribution and $\left(\frac{{G_\phi}^{real}}{({\sigma_\phi})^{real}}\right)^2$ has a non-central chi-squared distribution because ${G_\phi}^{real}$ has a non-zero mean.
Moreover, for the correlation between ${G_\phi}^{real}$ and ${G_\phi}^{img}$, which we denote by ρ, Lemma 2 holds

Lemma 2: It holds that

$$\rho = \frac{E\left|\left({G_\phi}^{real} - {\mu_\phi}^{real}\right)\left({G_\phi}^{img} - {\mu_\phi}^{img}\right)\right|}{{\sigma_\phi}^{real}{\sigma_\phi}^{img}} = 0\,, \quad (10)$$

which indicates that ${G_\phi}^{real}$ and ${G_\phi}^{img}$ are uncorrelated.
Proof: See Appendix B.

As a result, given the fact that two uncorrelated Gaussian distributions are also independent, we conclude that ${G_\phi}^{real}$ and ${G_\phi}^{img}$ are approximately independent random variables for adequately large S, even though they both depend on ϕ_s.

Proposition 1: For an adequately large S and by using (6) and Lemma 2, the CDF of G_ϕ, which we denote by $F_{G_\phi}(g)$, can be approximated as

$$F_{G_\phi}(g) \approx \int_0^g \left[1 - 2Q\left(\frac{\sqrt{g-y}}{({\sigma_\phi})^{real}}\right)\right] \frac{e^{\frac{-y}{2\left({\sigma_\phi}^2\right)^{img}}}}{({\sigma_\phi})^{img}\sqrt{2\pi y}} dy. \quad (11)$$

Proof: See Appendix C.

B. Computation of the maximum phase error tolerance

Let us now assume a target data rate, denoted by R_t, as a system-design requirement. Due to imperfect phase synchronization and the resulting randomness in the achieved beamforming gain, there is a probability that the achieved rate falls below the target, which should be kept within the system design requirements, by achieving the maximum phase inaccuracy tolerance. For a given position estimation error, the corresponding inaccuracy in phase is given by $\Delta\phi = \frac{2\pi\Delta d}{\lambda}$. We now analyze the maximum value of ϕ, in the uniform distribution of ϕ_s, that achieves the target rate.

Given R_t, we can compute the maximum tolerable phase error ϕ by setting a condition for the CDF of the normalized main lobe gain as

$$P\left(R_\phi < \alpha R_t\right) < \beta, \quad (12)$$

where R_ϕ is the achieved data rate given a maximum phase error of ϕ, and $\alpha, \beta \in (0,1)$. Typically, we expect α to be close to 1 and β to be close to 0. From Shannon's formula and by assuming a high-SNR regime with unit noise power we have the following equation for the rate without phase error.

$$R_t = \log_2\left(g(0)^2 NS\right) \quad (13)$$

Considering a reduced gain with phase error, we can write the compromised achievable data rate as $\alpha R_t = \log_2\left(G_\phi g(0)^2 NS\right)$, which implies that the corresponding normalized gain is given by

$$\begin{aligned} G_\phi &= \frac{2^{\alpha R_t}}{g(0)^2 NS} \\ &= \left|g(0)^2 NS\right|^{\alpha-1} \end{aligned} \quad (14)$$

Then (12) can be re-defined as

$$P\left(G_\phi < \left|g(0)^2 NS\right|^{\alpha-1}\right) < \beta \quad (15)$$

Therefore, the maximum allowable ϕ satisfies the following

$$\begin{aligned} &F_{G_\phi}\left(\left|g(0)^2 NS\right|^{\alpha-1}\right) = \beta \\ &F_{G_\phi}\left(\left|g(0)^2 NS\right|^{\alpha-1}\right) - \beta = 0 \end{aligned} \quad (16)$$

If we let $f(\phi) = F_{G_\phi}\left(\left|g(0)^2 NS\right|^{\alpha-1}\right) - \beta$, the Newton-Raphson method could be applied to find ϕ, such that $f(\phi) = 0$. Although the derivative of the function cannot be expressed in terms of elementary functions, numerical solutions can be obtained. We start with an initial ϕ, and iteratively update the value as follows

$$\phi_{n+1} = \phi_n - \frac{f(\phi_n)}{f'(\phi_n)}, \quad (17)$$

ϕ_n is the estimate at the n^{th} iteration, which continues until $|f(\phi_n)|$ is within a small error bound.

$$\phi_{est} = \phi_n, \quad \text{such that} \quad \begin{matrix} |f(\phi_{n-1})| > \epsilon \\ |f(\phi_n)| \le \epsilon \end{matrix}, \quad (18)$$

where ϕ_{est} is the estimated phase, and ϵ is the error bound.

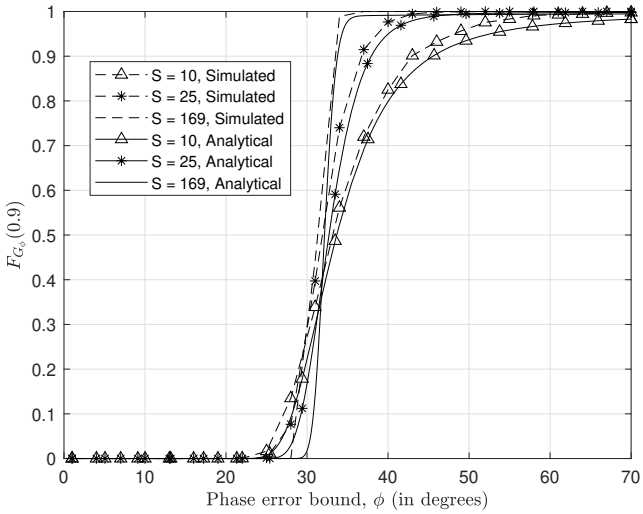

Fig. 1: $F_{G(\phi)}(0.9)$ vs ϕ.

IV. Simulation results

Let us now validate the analytical frameworks of (11) and (18) by comparing it against Monte-Carlo simulations. Towards this, Fig. 1 illustrates $F_{G(\phi)}(0.9)$ for ϕ in the range

	S = 10			S = 25			S = 169		
Target (α, β)	ϕ_{est} (in degrees)	Simulated (α, β) pairs at ϕ_{est}	d_{err} (in mm)	ϕ_{est} (in degrees)	Simulated (α, β) pairs at ϕ_{est}	d_{err} (in mm)	ϕ_{est} (in degrees)	Simulated (α, β) pairs at ϕ_{est}	d_{err} (in mm)
(0.9, 0.05)	64	$(0.9, 0.053)$	1.78	71	$(0.9, 0.045)$	1.97	85	$(0.9, 0.046)$	2.36
(0.95, 0.05)	46	$(0.95, 0.0501)$	1.28	51	$(0.95, 0.044)$	1.41	62	$(0.95, 0.053)$	1.72
(0.99,0.05)	21	$(0.99, 0.048)$	0.58	23	$(0.99, 0.037)$	0.64	29	$(0.99, 0.058)$	0.81
(0.9, 0.01)	60	$(0.9, 0.014)$	1.67	68	$(0.9, 0.013)$	1.89	84	$(0.9, 0.019)$	2.33
(0.95, 0.01)	43	$(0.95, 0.013)$	1.19	49	$(0.95, 0.009)$	1.36	61	$(0.95, 0.021)$	1.69
(0.99,0.01)	20	$(0.99, 0.017)$	0.56	22	$(0.99, 0.013)$	0.61	28	$(0.99, 0.012)$	0.78

TABLE I: Estimated phase error, ϕ_{est} at different (ϕ, β) pairs for 10, 25 and 169 number of satellites. d_{err} represents the position error computed from ϕ_{est}, at 30GHz frequency.

$(-\pi, \pi)$ and for $S = 10, 25, 169$ and $N = 49$. As we observe from Fig. 1, there is a close match of the analytical framework with the simulations, which substantiates the importance of the analytical framework, even for low S.

In addition, the maximum tolerable phase error estimated by (18) for a set of pairs of (α, β), denoted by ϕ_{est} is shown in Table I. For comparison, we obtained (α, β) pairs evaluated at ϕ_{est} by generating random realizations of the normalized gains. The values show that the simulated (ϕ, β) pairs are close to the target (α, β), indicating that ϕ_{est} is fairly accurate. To elaborate the results more vividly, let us consider a high rate network providing 100 Mbps. By referring to Table I, we see that at $(0.9, 0.05)$, ϕ_{est} for a swarm of 10 satellites is 64^0. The interpretation is as follows; if the phase error has a distribution of $U(-\phi, \phi)$, where $\phi \leq 64^0$, then we can guarantee that there is a less than 0.05 probability that the rate is under 90Mpbs. As pointed out in previous works, higher number of satellites are more tolerant of phase errors. This is because as the number of satellites increases, the compromised normalized gain tends to concentrate around the average by law of large numbers. As a result, the probability of the gain falling below a threshold decreases. However, this does not lead to an increased average normalized gain as well. In fact, it can be observed that it decreases slightly with increasing number of satellites.

$$E(G_\phi) = E\left|\left({G_\phi}^{real}\right)^2\right| + E\left|\left({G_\phi}^{img}\right)^2\right| = \left({\sigma_\phi}^2\right)^{real} + \left({\mu_\phi}^2\right)^{real} + \left({\sigma_\phi}^2\right)^{img} + \left({\mu_\phi}^2\right)^{img} \tag{19}$$

By substituting (7) and (8) into (19) and by using the first derivative test, it is straightforward to see that $E(G_\phi)$ monotonically decreases with S.

Additionally, given ϕ_{est}, the tolerable position estimation error is also computed for mmWave 30 GHz carrier frequency as $d_{err} = \frac{\phi_{est} \times \lambda}{2\pi}$ as the worst case scenario. We see from TABLE I that in order to achieve a data rate of above 90% of the target, the accuracy in position estimation should be in the range of millimeters. This becomes even stricter for higher frequencies in future high-bandwidth communications.

V. CONCLUSION

In this paper, we analyzed the effect of error in phase and position estimation on beamforming gain in distributed swarm of LEO satellites. We laid out a framework for computing the distribution/spread of the main lobe gain under imperfect phase synchronization, and validated the results of the analysis by comparing with simulations from random realizations. Referring to the results, it was found that mmWave communication requires inter-satellite ranging accuracy in order of millimeters to avoid significant loss in data rate. As the number of satellites increases, so does the allowable error in phase. This analysis can be extended in future work to analytically derive the interference statistics due to imperfect phase synchronization in a multi-user transmission scenario from the satellite swarm.

ACKNOWLEDGEMENTS

ETHER project has received funding from the Smart Networks and Services Joint Undertaking (SNS JU) under the European Union's Horizon Europe research and innovation programme under Grant Agreement No. 101096526. Views and opinions expressed are however those of the author(s) only and do not necessarily reflect those of the European Union. Neither the European Union nor the granting authority can be held responsible for them.

APPENDIX

A. *Proof of Lemma 1:*

It holds:

$${\mu_\phi}^{real} = \int_{-\phi}^{\phi} \frac{\sum_{s=1}^{s=S} \cos(\phi_s)}{S} = \left.\frac{\sum_{s=1}^{s=S} \sin(\phi_s)}{S}\right|_{-\phi}^{\phi} = \frac{\sin(\phi)}{\phi}, \tag{20}$$

$${\mu_\phi}^{img} = \int_{-\phi}^{\phi} \frac{\sum_{s=1}^{s=S} \sin(\phi_s)}{S} = \left.\frac{\sum_{s=1}^{s=S} -\cos(\phi_s)}{S}\right|_{-\phi}^{\phi} = 0 \tag{21}$$

$$\begin{aligned}\left({\sigma_\phi}^2\right)^{real} &= \frac{1}{S^2}\sum_{s=1}^{s=S} \sigma^2_{\cos\phi_s} \\ &= \frac{1}{2\phi S}\int_{-\phi}^{\phi}\left(\cos\phi_s - \left(\frac{\sin\phi}{\phi}\right)\right)^2 d\phi_s, \\ &= \frac{1}{S}\left[\frac{1}{2} + \frac{\sin(2\phi)}{4\phi} - \left(\frac{\sin(\phi)}{\phi}\right)^2\right]\end{aligned} \tag{22}$$

$$\begin{aligned}\left(\sigma_\phi{}^2\right)^{img} &= \frac{1}{S^2}\sum_{s=1}^{s=S}\sigma^2_{\sin\phi_s}\\ &= \frac{1}{2\phi S}\int_{-\phi}^{\phi} 1-(\cos\phi_s)^2\, d\phi_s, \\ &= \frac{1}{S}\left[\frac{1}{2}-\frac{\sin(2\phi)}{4\phi}\right]\end{aligned} \tag{23}$$

B. *Proof of Lemma 2:*

It holds that

$$\begin{aligned}\rho &= \frac{E\left|\left(G_\phi{}^{real}-\mu_\phi{}^{real}\right)\left(G_\phi{}^{img}-\mu_\phi{}^{img}\right)\right|}{\sigma_\phi{}^{real}\sigma_\phi{}^{img}}\\ &= \frac{E\left|\left(\frac{\sum_{s=1}^{s=S}\cos(\phi_s)}{S}-\frac{\sin(\phi)}{\phi}\right)\left(\frac{\sum_{s=1}^{s=S}\sin(\phi_s)}{S}\right)\right|}{\sigma_\phi{}^{real}\sigma_\phi{}^{img}}\end{aligned} \tag{24}$$

For the numerator of (24) it holds

$$\begin{aligned}&E\left|\left(\frac{\sum_{s=1}^{s=S}\cos(\phi_s)}{S}-\frac{\sin(\phi)}{\phi}\right)\left(\frac{\sum_{s=1}^{s=S}\sin(\phi_s)}{S}\right)\right|\\ &= \frac{1}{S^2}E\left|\sum_{s=1}^{s=S}\cos(\phi_s)\sum_{s=1}^{s=S}\sin(\phi_s)\right| - \frac{\sin(\phi)}{\phi}E\left|\sum_{s=1}^{s=S}\sin(\phi_s)\right|\end{aligned} \tag{25}$$

The second term of (25) equals zero. We now proceed with the analysis of the first term. It holds

$$\begin{aligned}&E\left|\sum_{s=1}^{s=S}\cos(\phi_s)\sum_{s=1}^{s=S}\sin(\phi_s)\right| = E\left|\sum_{n=1}^{n=S}\sum_{m=1}^{m=S}\cos(\phi_n)\sin(\phi_m)\right|\\ &\overset{(a)}{=} \frac{1}{4\phi}\sum_{s=1}^{s=S}\int_{-\phi}^{\phi}\sin(2\phi_s)d(\phi_s) \;+\\ &\frac{1}{8\phi^2}\sum_{n=1}^{n=S}\sum_{\substack{m=1\\ m\neq n}}^{m=S}\int_{-\phi}^{\phi}\int_{-\phi}^{\phi}\left|\sin(\phi_n+\phi_m)-\sin(\phi_n-\phi_m)\right|\\ &d(\phi_n)d(\phi_m) = 0,\end{aligned} \tag{26}$$

where in (a) we use

$$\cos(\phi_n)\sin(\phi_m) = \frac{1}{2}\left|\sin(\phi_n+\phi_m)-\sin(\phi_n-\phi_m)\right|. \tag{27}$$

C. *Proof of Proposition 1:*

To derive the cumulative distribution function in equation (11), we make this simplification in notation. let $X = \left(\frac{G_\phi{}^{real}}{(\sigma_\phi)^{real}}\right)^2$, $\hat{X} = \left(\sigma_\phi{}^2\right)^{real}X$, and $Y = \left(\frac{G_\phi{}^{img}}{(\sigma_\phi)^{img}}\right)^2$, $\hat{Y} = \left(\sigma_\phi{}^2\right)^{img}Y$. Then we have $G_\phi = Z = \left(\sigma_\phi{}^2\right)^{real}X + \left(\sigma_\phi{}^2\right)^{img}Y = \hat{X}+\hat{Y}$. The CDF of X and PDF of Y are given below as they are useful in deriving the CDF of Z.

$$F_X(x) = \left[1-Q\left(\sqrt{x}-\frac{\mu_\phi{}^{real}}{(\sigma_\phi)^{real}}\right)-Q\left(\sqrt{x}+\frac{\mu_\phi{}^{real}}{(\sigma_\phi)^{real}}\right)\right]$$

$$P_Y(y) = \frac{e^{\frac{-y}{2}}}{\sqrt{2\pi y}}$$

$$\begin{aligned}F_Z(z) = P(Z\le z) &= \int_0^z\int_0^{z-\hat{y}} P_{\hat{X}}(\hat{x})\,P_{\hat{Y}}(\hat{y})\,d\hat{x}d\hat{y}\\ &= \int_0^z\int_0^{z-\hat{y}}\frac{d}{d\hat{x}}\left[F_X\left(\frac{\hat{x}}{(\sigma_\phi{}^2)^{real}}\right)\right]\\ &\quad\times\frac{d}{d\hat{y}}\left[F_Y\left(\frac{\hat{y}}{(\sigma_\phi{}^2)^{img}}\right)\right]d\hat{x}d\hat{y}\\ &= \int_0^z F_X\left(\frac{z-\hat{y}}{(\sigma_\phi{}^2)^{real}}\right)\frac{1}{(\sigma_\phi{}^2)^{img}}P_Y\left(\frac{\hat{y}}{(\sigma_\phi{}^2)^{img}}\right)d\hat{y}\\ &= \int_0^z\left[1-2Q\left(\frac{\sqrt{z-\hat{y}}}{(\sigma_\phi)^{real}}\right)\right]\frac{e^{\frac{-\hat{y}}{2\left(\sigma_\phi{}^2\right)^{img}}}}{(\sigma_\phi)^{img}\sqrt{2\pi\hat{y}}}d\hat{y}\end{aligned} \tag{28}$$

By a simple change of variables, we obtain (11).

REFERENCES

[1] M. M. Azari et al., "Evolution of Non-Terrestrial Networks From 5G to 6G: A Survey," in IEEE Communications Surveys & Tutorials, vol. 24, no. 4, pp. 2633-2672, Fourthquarter 2022.

[2] Merlano Duncan, J.C. Ha, Vu Krivochiza, Jevgenij Palisetty, Rakesh Eappen, Geoffrey Vasquez, Juan Martins, Wallace Chatzinotas, Symeon Ottersten, Björn. (2023). Harnessing the Power of Swarm Satellite Networks with Wideband Distributed Beamforming.

[3] D. Tuzi, T. Delamotte and A. Knopp, "Satellite Swarm-Based Antenna Arrays for 6G Direct-to-Cell Connectivity," in IEEE Access, vol. 11, pp. 36907-36928, 2023, doi: 10.1109/ACCESS.2023.3257102.

[4] L. M. Marrero et al., "Architectures and Synchronization Techniques for Distributed Satellite Systems: A Survey," in IEEE Access, vol. 10, pp. 45375-45409, 2022, doi: 10.1109/ACCESS.2022.3169499.

[5] J. A. Nanzer, S. R. Mghabghab, S. M. Ellison and A. Schlegel, "Distributed Phased Arrays: Challenges and Recent Advances," in IEEE Transactions on Microwave Theory and Techniques, vol. 69, no. 11, pp. 4893-4907, Nov. 2021, doi: 10.1109/TMTT.2021.3092401.

[6] J. A. Nanzer, R. L. Schmid, T. M. Comberiate and J. E. Hodkin, "Open-Loop Coherent Distributed Arrays," in IEEE Transactions on Microwave Theory and Techniques, vol. 65, no. 5, pp. 1662-1672, May 2017, doi: 10.1109/TMTT.2016.2637899.

[7] I. Dagres, A. Polydoros and A. Moustakas, "Performance Analysis of Distributed Beamforming in Wireless Networks: The Effect of Synchronization and Doppler spread," MILCOM 2021 - 2021 IEEE Military Communications Conference (MILCOM), San Diego, CA, USA, 2021, pp. 957-962, doi: 10.1109/MILCOM52596.2021.9653042.

[8] H. Ochiai, P. Mitran, H. V. Poor and V. Tarokh, "Collaborative beamforming for distributed wireless ad hoc sensor networks," in IEEE Transactions on Signal Processing, vol. 53, no. 11, pp. 4110-4124, Nov. 2005, doi: 10.1109/TSP.2005.857028.

[9] R. Mudumbai, G. Barriac and U. Madhow, "On the Feasibility of Distributed Beamforming in Wireless Networks," in IEEE Transactions on Wireless Communications, vol. 6, no. 5, pp. 1754-1763, May 2007, doi: 10.1109/TWC.2007.360377.

[10] G. Bacci, R. D. Gaudenzi, M. Luise, L. Sanguinetti and E. Sebastiani, "Formation-of-Arrays Antenna Technology for High-Throughput Mobile Nonterrestrial Networks," in IEEE Transactions on Aerospace and Electronic Systems, vol. 59, no. 5, pp. 4919-4935, Oct. 2023, doi: 10.1109/TAES.2023.3244773.

[11] A. Papoulis, "Probability, Random Variables, and Stochastic Processes," 3rd Edition, McGraw-Hill, New York, 1991.